Published in final edited form as:
Eur J Cardiothorac Surg. 2010 September ; 38(3): 340–349. doi:10.1016/j.ejcts.2010.02.011.

HOW DO ANNULOPLASTY RINGS AFFECT MITRAL LEAFLET DYNAMIC MOTION?

Wolfgang Bothe[*], **John-Peder Escobar Kvitting**[*], **Julia C. Swanson**[*], **Serdar Göktepe**[$], **Kathy N. Vo**[*], **Neil B. Ingels Jr.**[*,#], and **D. Craig Miller**[*]

[*] Department of Cardiothoracic Surgery, Stanford University School of Medicine, Stanford, California

[$] Department of Mechanical Engineering, Stanford University, Stanford, California

[#] Laboratory of Cardiovascular Physiology and Biophysics, Research Institute of the Palo Alto Medical Foundation, Palo Alto, California

Abstract

Objectives—To define the effects of annuloplasty rings (ARs) on the dynamic motion of anterior and posterior mitral leaflets (AML, PML).

Methods—Sheep had radiopaque markers inserted: 8 around the mitral annulus, four along the central meridian (from edge to annulus) of the AML (#A_1–#A_4) and one on the PML edge (#P_1). True-sized Edwards Cosgrove (COS, n=12), St Jude RSAR (n=12), Carpentier-Edwards Physio (PHYSIO, n=12), Edwards IMR ETlogix (ETL, n=10) or Edwards GeoForm (GEO, n=12) ARs were implanted in a releasable fashion. Under acute open-chest conditions, 4-D marker coordinates were obtained using biplane videofluoroscopy with the ARs inserted (COS, RSAR, PHYSIO, ETL, GEO) and after release (COS-CONTROL, RSAR-CONTROL, PHYSIO-CONTROL, ETL-CONTROL, GEO-CONTROL). AML and PML excursions were calculated as the difference between minimum and maximum angles between the central mitral annular septal-lateral chord and the anterior mitral leaflet edge markers ($\alpha_{1exc} - \alpha_{4exc}$) and PML edge marker ($\beta_{1exc}$) during the cardiac cycle.

Results—Relative to CONTROL, 1.) RSAR, PHYSIO, ETL and GEO increased excursion of the AML annular (α_{4exc}: 13±6° *vs.* 16±7°*, 16±7° *vs.* 23±10°*, 12±4° *vs.* 18±9°*, 15±1° *vs.* 20±9°*, respectively) and belly region (α_{2exc}: 41±10° *vs.* 45±10°*, 42±8° *vs.* 45±6°, n.s., 33±13° *vs.* 42±14°*, 39±6° *vs.* 44±6°*, respectively, α_{3exc}: 24±9° *vs.* 29±11°*, 28±10° *vs.* 33±10°*, 16±9° *vs.* 21±12°*, 25±7° *vs.* 29±9°*, respectively), but not of the AML edge (α_{1exc}: 42±8° *vs.* 44±8°, 43±8° *vs.* 41±6°, 42±11 *vs.* 46±10°, 39±9° *vs.* 38±8°, respectively, all n.s.). COS did not affect AML excursion (α_{1exc}: 40±8° *vs.* 37±8°, α_{2exc}: 43±9° *vs.* 41±9°, α_{3exc}: 27±11° *vs.* 27±10°, α_{4exc}: 18±8° *vs.* 17±7°,, all n.s.). 2.) PML excursion (β_{1exc}) was reduced with GEO (53±5° *vs.* 43±6°*), but unchanged with COS, RSAR, PHYSIO or ETL (53±13° *vs.* 52±15°, 50±13° *vs.* 49±10°, 55±5° *vs.* 55±7°, 52±8° *vs.* 58±6°, respectively, all n.s). *=$p<0.05$

Address for correspondence: D. Craig Miller, M.D., Department of Cardiothoracic Surgery, Falk Cardiovascular Research Center, Stanford University School of Medicine, Stanford, California 94305-5247, 001.650.725.3826 FAX 001.650.725.3846, dcm@stanford.edu.

Presented at the 23rd Annual Meeting of the European Association of Cardio-Thoracic Surgery, Vienna, Austria, October 17th–21st 2009

Conclusions—RSAR, PHYSIO, ETL and GEO rings, but not COS, increase AML excursion of the AML annular and belly region suggesting higher anterior mitral leaflet bending stresses with rigid rings, which potentially could be deleterious with respect to repair durability. The decreased PML excursion observed with GEO could impair LV filling. Clinical studies are needed to validate these findings in patients.

Keywords

Mitral valve; annuloplasty rings; leaflet dynamics

INTRODUCTION

Mitral valve repair has become the gold-standard treatment for patients with mitral regurgitation and most commonly includes the implantation of an annuloplasty ring [1] which invariably changes the geometry, dynamics and force distribution of the mitral annulus [2–4]. Such annular changes have been demonstrated to perturb the geometry of the mitral leaflets during valve closure [5,6], which has been associated with alterations in physiological stress patterns acting on the leaflets and suboptimal repair durability [7,8]. The effects of annuloplasty rings on mitral leaflet dynamics are, however, less clear. While some studies suggest ring-induced changes in mitral leaflet dynamic motion [9,10], other studies do not demonstrate alterations in leaflet dynamics with annuloplasty rings [11]. A better understanding of the effects of annuloplasty rings on mitral leaflet dynamic motion is important because such alterations could affect physiological leaflet stress distribution and, thus, repair durability.

Our goal was to assess the effects of five different annuloplasty ring types (Cosgrove-Edwards band, St. Jude Medical rigid saddle ring, Carpentier-Edwards Physio, Edwards IMR ETlogix and Edwards GeoForm) on mitral leaflet dynamic motion in an experimental ovine model using four-dimensional radiopaque marker tracking.

MATERIALS AND METHODS

Surgical preparation

Fifty eight adult, Dorsett-hybrid, male sheep (49±5kg) were premedicated with ketamine (25mg/kg intramuscularly), anesthetized with sodium thiopental (6.8mg/kg intravenously), intubated and mechanically ventilated with inhalational isoflurane (1.0–2.5%). All animals received humane care in compliance with the *Principles of Laboratory Animal Care* formulated by the National Society of Medical Research and the *Guide for Care and Use of Laboratory Animals* prepared by the National Academy of Sciences and published by the National Institute of Health (DHEW NIHG publication 85-23, revised 1985). This study was approved by the Stanford University Medical Center Laboratory Research Animal Review committee and conducted according to Stanford University policy.

Through a left thoracotomy, 13 radiopaque markers were implanted to silhouette the left ventricle (LV) at the cross-section points of two equally spaced longitudinal and three equatorial meridians and the LV apex as described earlier [12]. Using cardiopulmonary bypass and cardioplegic arrest, 8 radiopaque markers were sewn to the mitral annulus and 4 markers were sewn to the central meridian of the anterior (#A_1-$_4$) and two to the posterior mitral leaflet (#P_1 and #P_2,Figure 1A). Five different annuloplasty ring models, the Cosgrove-Edwards band (COS, Edwards Lifesciences, Irvine, CA, USA, n=12), St. Jude Medical rigid saddle ring (RSAR, St. Jude Medical Inc, St. Paul, MN, USA, n=12), Carpentier-Edwards Physio (PHYSIO, n=12), Edwards IMR ETlogix (ETL, n=10) and

Edwards GeoForm (GEO, n=12, all three Edwards Lifesciences, Irvine, CA, USA) were implanted in a releasable fashion as described earlier [13].

All annuloplasty rings were "true-sized" (*i.e.*, the size was chosen as assessed with the sizer provided by the manufacturer) by determining the height and the entire area of the entire anterior mitral leaflet. As all animals had similarly sized leaflets, all received size 28 rings. After weaning from cardiopulmonary bypass, the sheep were transferred to the experimental catheterization laboratory under acute open chest conditions.

Data acquisition

Videofluoroscopic images (60 Hz) of all radiopaque markers were acquired using biplane videofluoroscopy (Philips Medical Systems, North America, Pleasanton, CA, USA). First, images were acquired with the ring inserted (COS, RSAR, PHYSIO, ETL, GEO). To acquire a data set for a parallel study, acute LV ischemia was then induced by tightening an encircling vessel loop around the circumflex branch of the left coronary artery for 90 sec. After the hemodynamics returned to baseline, the locking sutures were pulled out and the ring was lifted away from the mitral annulus toward the left atrial roof using drawstrings. A third data acquisition was performed and images were acquired with the ring released (COS-Control, RSAR-Control, PHYSIO-Control, ETL-Control, GEO-Control). Data from mitral annular and leaflet geometry using this dataset have been published earlier [13,14].

Four-dimensional marker coordinates were obtained as described previously [15]. Data from 3 consecutive hemodynamically stable beats in normal sinus rhythm were averaged and analyzed. End-systole was defined as the videofluoroscopic frame immediately preceding the peak negative rate of LV pressure change ($-dP/dt_{max}$) and end-diastole as the videofluoroscopic frame containing the peak of the R-wave on the ECG. Distance between anterior and posterior leaflet edge markers ($\#A_1$ and $\#P_1$) were computed throughout the cardiac cycle. Mid-systole was defined from these distance values as: ((Closure 2 − Closure 1)/2) + Closure 1, where Closure 1 was the time of leaflet closure (immediately after the end of diastolic filling) and Closure 2 was the time immediately before valve opening.

Data analysis

Hemodynamics—Instantaneous LV volume was computed from the epicardial LV markers using a space-filling multiple tetrahedral volume method [16]. Hemodynamic data were calculated from marker derived instantaneous LV volumes and analog LV pressures as described earlier [15].

Mitral leaflet motion

Valve opening: In order to determine the effects of annuloplasty rings on mitral valve opening, maximum values from plotted distance curves between markers $\#A_1$ and $\#P_1$ were extracted and defined as maximum valve opening.

Regional leaflet dynamic motion: In order to assess the effects of the implanted rings on regional anterior as well as posterior mitral leaflet motion, angles between anterior and posterior leaflet markers ($\#A_1$–$\#A_4$ and $\#P_1$–$\#P_2$, respectively) and the central mitral annular septal lateral cord (#17–#19) were calculated throughout the cardiac cycle as $\alpha_{1–4}$ and β_1–β_2, respectively (Figure 1B). Minimum and maximum values were extracted from plotted curves. Minimum values were subtracted from maximum values to determine anterior and posterior mitral leaflet excursion (Figure 1C).

Leaflet opening and closing velocity: The slopes were calculated from plotted regional leaflet angle curves (α_{1-4}, β_1 and β_2) and maximum and minimum values were extracted to describe regional leaflet closing and opening velocity (VC_{max} and VO_{max}, respectively).

Distance of anterior mitral leaflet edge to LV septum: The distance between the anterior mitral leaflet edge marker (#A_1) and the septal equatorial LV marker was calculated (Figure 1D).

Mitral leaflet geometry—In order to describe the geometry of the anterior and posterior mitral leaflets along their central leaflet meridian during valve closure and LV filling, leaflet marker 3-D coordinates were transformed into a right-handed Cartesian coordinate system, with origin at the mitral annular saddlehorn marker (#17, Figure 1A), positive y-axis passing through the LV apex marker, positive x-axis orthogonal to the y-axis with the x-y plane containing the mitral annular mid-lateral marker (#19, Figure 1A), with positive z-axis directed toward the posterior commissure. Marker x-y coordinates were plotted at mid-systole and at maximum valve opening to display leaflet shape along the central leaflet meridians.

Statistical Analysis—Data are reported as mean ± 1 SD unless otherwise stated. Control data (COS-Control, RSAR-Control, PHYSIO-Control, ETL-Control, GEO-Control) and data with the respective ring inserted (COS, RSAR, PHYSIO, ETL, GEO) were compared using one-way repeated measures ANOVA with a Holm-Sidak posthoc test (Sigmastat 3.5, Systat Software, Inc, San Jose, CA, USA). A p-value of less than 0.05 was considered to be statistically significant.

RESULTS

Hemodynamics

Group mean hemodynamic indices are shown in Table 1. No significant differences were found between ring and control states in all five groups with respect to heart rate, LV dP/dt (except for Cosgrove, where dP/dt was slightly higher compared to Control) and LVEDV.

Mitral leaflet motion

Valve opening—Table 2 displays mitral valve opening in the five annuloplasty ring groups with and without the respective rings inserted. Compared to the Control state, all rings decreased maximum leaflet separation, *i.e.,* valve opening; for RSAR, this trend was statistical insignificant (p=0.073).

Regional leaflet dynamic motions—Table 2 also shows the regional anterior and posterior leaflet excursion as well as leaflet opening and closing velocities in the five groups. While regional leaflet excursion increased in the belly (α_2 and α_3)and annular region (α_4)with all rigid, complete rings, RSAR, PHYSIO, ETL and GEO (although insignificantly for α_2 with PHYSIO: 42±8° *vs.* 45±8°, n.s.), none of these three rings affected the excursion of α_1. COS did not affect anterior mitral leaflet excursion (excursion of α_1 –α_4). Posterior mitral leaflet edge excursion (excursion of β_1) was reduced with GEO, but unchanged with COS, RSAR, PHYSIO. or ETL. In order to illustrate whether the observed changes in leaflet excursion were due to changes in minimum or maximum leaflet angles, or both, Figure 2A–F shows the maximum and minimum angles for the anterior (Figure 2A–D) and posterior (Figure 2E–F) leaflets for all five groups with and without the respective rings. The increased excursion of α_{2-4} found with RSAR, PHYSIO, ETL and GEO (Table 2) was accompanied with increases in maximum values of angle α_2 and α_3. The minimum values of angle α_2 did not change with RSAR, PHYSIO and ETL, but increased with GEO.

Furthermore, ETL and GEO increased minimum values of α_3 and α_4. The decreased excursion of the posterior mitral leaflet (excursion of β_1 and β_2) found with GEO was due to an increase in minimum angles, which was greater than the increase in maximum angles (Figure 2E and F).

Leaflet opening and closing velocity—The complete, rigid rings (RSAR, PHYSIO, ETL and GEO), but not COS, increased both, VO_{max} and VC_{max} in the belly region of the anterior mitral leaflet near the annulus (α_3) as compared to Control (Table 2, not significant for VC_{max} of PHYSIO: 42±14 *vs.* 48±15 deg/s, p=0.104, F=3.1). These rings also increased VC_{max} predominately in the anterior mitral leaflet belly region closer to the edge (VC_{max} of α_2). Only ETL and GEO affected VC_{max} or VO_{max} of the posterior mitral leaflet edge (β_1). While ETL increased VO_{max} and VC_{max} ofβ_1, GEO decreased VO_{max} of β_1..

Distance of anterior mitral leaflet edge to LV septum—Compared to Control, PHYSIO, ETL and GEO, but not RSAR or COS, decreased the distance of the anterior mitral leaflet edge and the LV septum at end-diastole (PHYSIO: 3.33±0.60cm *vs.* 3.01±0.59cm, p=.001, F=18.9, ETL: 3.57±0.34cm *vs.* 3.27±0.36cm, p=.015, F=9.0, GEO: 3.12±0.67cm *vs.* 2.83±0.46cm, p=.046, F=5.2, RSAR: 3.12±0.67cm *vs.* 3.03±0.67cm, n.s., F=2.0, COS: 3.09±0.70cm *vs.* 3.09±0.71cm, n.s., F=0). Figure 3A–E shows curves of the distance between the anterior mitral leaflet edge marker ($\#A_1$) and the LV septum, as well as the distance between the anterior and posterior mitral leaflet edge markers ($\#A_1$ and $\#P_1$) for all five groups with and without ring insertion plotted with t=0 at end-diastole. COS and RSAR did not affect the anterior mitral leaflet edge to LV septum distance during the closing motion of the valve, whereas PHYSIO, ETL and GEO result in a smaller distance while the valve closes. GEO, but not COS, RSAR, PHYSIO or ETL resulted in a smaller distance of the anterior mitral leaflet edge to the LV septum when the valve was tightly closed.

Mitral leaflet geometry

Figure 4A–E shows the mean 2-D positions of the anterior and posterior mitral leaflet markers as well as the mitral annular markers #17 and #19 plotted onto an X-Y plane for all five ring groups at mid-systole and maximum valve opening with and without the ring inserted. While all rings reduced mitral annular dimensions, COS, RSAR, PHYSIO or ETL implantation did not affect the anterior mitral leaflet geometry along the central meridian at mid-systole, or at maximum opening. GEO implantation resulted in a more acute angle of the anterior mitral leaflet edge. The posterior mitral leaflet geometry along the central meridian appeared similar to the control state in all ring groups both at mid-systole and maximum valve opening.

Video 1 shows an animation of the mean 2-D positions of the markers for all five ring groups during the cardiac cycle. The subtle increases in the excursion of the leaflet annulus and belly region with RSAR, PHYSIO, ETL and GEO (α_2, see above) can be appreciated as well as the drastic changes in mitral annular geometry and dynamics.

DISCUSSION

This study reports, for the first time, the effects of conventional as well as recently-designed new annuloplasty rings on anterior and posterior mitral leaflet dynamics using a releasable ring insertion experimental preparation. The principal findings of this study were: (1.) All five ring types reduced maximum valve opening despite true-sizing; (2.) RSAR, PHYSIO, ETL and GEO rings, but not COS, increased the excursion of the anterior mitral leaflet annular (α_4) and belly (α_2 and α_3) region, while none of the rings affected excursion of the

anterior mitral leaflet edge (α_1); (3) GEO decreased the excursion of the posterior mitral leaflet edge (β_1), while COS, RSAR, PHYSIO and ETL did not affect posterior leaflet edge motion; (4) RSAR, PHYSIO, ETL and GEO increased both opening and closing velocities of the anterior leaflet belly (α_3); (5) Only GEO changed the geometry of the central meridian of the anterior mitral leaflet during valve closure, with the edge region bending more acutely (concave to the LV); (6) PHYSIO, ETL and GEO, but not COS and RSAR decreased the distance of the anterior mitral leaflet edge to the LV septum at end-diastole.

The finding of a reduction in maximum valve opening, regardless of ring type, was surprising. Although a smaller effective mitral orifice area due to ring implantation has been described [17], the rings in the present study were true-sized and implanted in healthy hearts with normal sized leaflets and mitral annuli. With regard to the physiologically shaped rings (i.e., COS, RSAR and PHYSIO) one may therefore expect that these rings do not impair maximum valve opening. Recently published analyses from our laboratory, however, have shown that even true-sized and physiologically shaped rings reduce mitral annular dimensions [14] especially during diastole when the dynamic annulus is largest [18]. The reduction in mitral valve opening observed is therefore most probably due to reductions in diastolic mitral annular dimensions caused by ring implantation.

In an earlier study, Timek *et al*. found no difference in anterior mitral leaflet excursion after implantation of a Physio ring in an ovine model [11]. In contrast, we observed an increase in the excursion of the anterior mitral leaflet belly with RSAR, PHYSIO, ETL and GEO. This discrepancy could result from the novel experimental setup (releasable ring methodology) used in this experiment. The releasable-ring methodology allows for paired comparison between “ring on” and “ring off” in the same heart and thus may enable us to detect more subtle differences. It is reasonable to speculate that such an increase in leaflet excursion results from subvalvular alterations caused by the annuloplasty ring implantation. Annuloplasty rings have been shown to decrease tethering length [19], *i.e.*, the distance from the papillary muscle tips to the saddle horn. In theory, these alterations may result in a slack of the strut chords which may lead to an increased leaflet excursion. Such an increase in leaflet excursion could result in greater bending stresses and, thus, potentially adversely affect long-term repair durability e.g by promoting a progression of degenerative leaflet or chordal disease after mitral valve repair as described by Marwick et al. [20]). Hypothetically, these adverse effects could be even more pronounced if smaller ring sizes were used than those assessed with the sizer (downsizing).

The posterior leaflet excursion was not affected by COS, RSAR or PHYSIO and increased with ETL. This is in contrast to earlier studies from our laboratory where restricted posterior leaflet motion was reported after implantation of a Medtronic Duran and an Edwards Physio ring [10]. This difference could again be due to our novel implantation methodology, where though the ring is in the same anatomical location the stitching technique was different from the conventional technique (see [13] for details). Furthermore, in the past data were acquired one week after ring implantation and early scarring may have impaired free leaflet mobility.

In contrast to all other rings, the GEO ring decreased the posterior leaflet excursion as well as the VO_{max} of the posterior leaflet edge (β_1). These effects could be due to the aggressive septal-lateral downsizing inherent in this ring model and/or due to its specific 3-D design: the 6mm elevation of the P-2 segment could exert a “folding effect” on the posterior leaflet which could impair free leaflet mobility. Regardless, our results suggest that the GEO ring could impair LV filling due to both, a decrease in posterior leaflet excursion (reduction of the effective mitral valve orifice) and a decrease in the VO_{max} of the posterior leaflet. This speculation, however, needs to be confirmed clinically.

The affect of annuloplasty rings on regional leaflet opening and closing velocities has not been previously reported. We found that the complete annuloplasty rings (RSAR, PHYSIO, ETL and GEO) increased both opening and closing velocities of the anterior leaflet belly (α_3, Table 2, increase in VC_{max} with PHYSIO did not reach statistical significance (42±14 *vs.* 48±15 deg/s, p=0.104, F=3.1). It could be possible that complete rings via alterations in regional mitral leaflet stiffness may accelerate the anterior leaflet opening and closing motion as postulated earlier by Sacks et al. [9].

In a recent analysis, Ryan *et al*. demonstrated that flat *versus* saddle-shaped annuloplasty rings have different affects on the curvature of the anterior mitral leaflet in the closed valve [5]. 3-D transesophageal echocardiography revealed that both a saddle-shaped ring (Medtronic 3-D Profile) and an Edwards Physio ring altered 3-D leaflet curvature. In the present study, we looked at geometric changes only along the central meridian of the leaflets. Ring implantation may have altered the geometry of the leaflets in the commissural regions. It is of note that the systolic position of the leaflet edge markers ($\#A_1$ and $\#P_1$) is only affected by the GEO ring, with the edge region bending more acutely (concave to the LV). This suggests that the effects of the saddle shape on the leaflet curvature may be less than previously assumed. The observed shape change with GEO appeared to be more due to a mechanical effect resulting from the inward displacement of the posterior mitral leaflet (note the dog-bone design of the GEO includes a disproportionate downsizing of the annular septal-lateral dimension by ~25–40% [21]) rather than as a consequence of alterations in the saddle-shape of the mitral annulus.

In our study, the distance between the edge of the anterior mitral leaflet and the LV septum at end-diastole and during the closing motion of the mitral valve were smaller with PHYSIO, ETL and GEO, but not with COS or RSAR. These findings could have implications with respect to the postoperative risk of systolic anterior leaflet motion. While many investigators hypothesize that increased flow velocities in the LV outflow tract create a Venturi effect [22] the precise mechanism is debated. Cross-sectional echocardiography of HCM patients demonstrated that systolic anterior leaflet motion began before ventricular ejection commenced [23]. Anterior and inward displacement of the papillary muscles [24], and elongation of the valve leaflets [25] have been reported as risk factors, both creating slack in the leaflets, allowing them to stray into the outflow tract. Consequently, a decreased distance between anterior mitral leaflet and LV septum at end-diastole may pose a risk for systolic anterior motion. Since this dimension was decreased with PHYSIO, ETL and GEO, which all have a flat anterior ring portion, preserving a saddle-shape by implanting the RSAR or COS could decrease the risk of postoperative systolic anterior mitral leaflet motion especially in patients with elongated leaflets and preserved LV function.

Limitations of the study

First, all rings were implanted in hearts with healthy LV's and normal leaflets, which is quite different than the usual clinical situation. The observations from this study can therefore not directly be extrapolated to patients with functional/ischemic mitral regurgitation. Furthermore, in patients with diseased (e.g., Barlow's) valves, the effects of these rings on leaflet motion and geometry may be different. In addition, no reconstructive procedures were performed on the posterior mitral leaflet (e.g. leaflet resection) which is common practice in patients with valve prolapse. Such procedures likely affect the dynamic motion of the posterior mitral leaflet. Second, the ring implantation method was different from current clinical practice. It cannot be estimated if and how this technique may have affected our results. We feel that the strength of this method (i.e., allowing paired comparisons), however, outweighs its potential drawbacks. Third, no mitral regurgitation occurred. Whether or not the 3-D shape of the ring implanted affects the risk of systolic anterior leaflet motion in patients has therefore yet to be proven. Fourth, data were only

reported from the central meridian of both leaflets. The effects of rings on leaflet motion close to the commissures therefore needs further investigation. Lastly, an ovine experimental model was used. Caution therefore needs to be exercised before extrapolating these findings to man.

Conclusions

All rigid, complete annuloplasty rings (RSAR, PHYSIO, ETL and GEO), but not the flexible incomplete band (COS), increased the excursion of the anterior mitral leaflet annular and belly region suggesting higher bending stresses with rigid rings, which potentially could be deleterious with respect to long-term repair durability. The decreased excursion of the posterior mitral leaflet observed with GEO might possibly hinder LV filling. Only GEO changed the geometry of the central meridian of the anterior mitral leaflet in the closed valve, most likely due to the radical inward displacement of the posterior mitral leaflet that results from its significant disproportionate septal-lateral downsizing. PHYSIO, ETL and GEO, but not COS and RSAR, decrease the end-diastolic distance of the anterior mitral leaflet to the LV septum, suggesting that preservation of a natural annular saddle shape could be important to minimize the risk of postoperative systolic anterior leaflet motion. Future clinical studies are needed to determine whether these findings translate to patients.

Video 1: Animation of mean 2-D positions of the anterior and posterior mitral leaflet markers and mitral annular markers #17 and #19 for all five ring groups during the cardiac cycle.

Supplementary Material

Refer to Web version on PubMed Central for supplementary material.

Acknowledgments

The authors gratefully acknowledge the expert help of Paul Chang, Maggie Brophy, Sigurd Hartnett, Eleazar P. Briones, Lauren R. Davis, and George T. Daughters (K6GT).

Supported by grants HL-29589 and HL-67025 from the National Heart, Lung and Blood Institute. Dr. Bothe was supported by the Deutsche Herzstiftung, Frankfurt, Germany.

Dr. Kvitting was funded by U.S. - Norway Fulbright Foundation and the Swedish Heart-Lung Foundation

Dr. Swanson was funded by Western States Affiliate American Heart Association Postdoctoral Fellowship Dr Miller is a consultant for Medtronic Heart Valve Division, Inc.

References

1. Enriquez-Sarano M, Akins CW, Vahanian A. Mitral regurgitation. Lancet 2009;373:1382–94. [PubMed: 19356795]
2. Glasson JR, Green GR, Nistal JF, Dagum P, Komeda M, Daughters GT, Bolger AF, Foppiano LE, Ingels NB Jr, Miller DC. Mitral annular size and shape in sheep with annuloplasty rings. J Thorac Cardiovasc Surg 1999;117:302–9. [PubMed: 9918972]
3. Jensen MO, Jensen H, Smerup M, Levine RA, Yoganathan AP, Nygaard H, Hasenkam JM, Nielsen SL. Saddle-shaped mitral valve annuloplasty rings experience lower forces compared with flat rings. Circulation 2008;118:S250–5. [PubMed: 18824763]
4. Yamaura Y, Yoshida K, Hozumi T, Akasaka T, Okada Y, Yoshikawa J. Three-dimensional echocardiographic evaluation of configuration and dynamics of the mitral annulus in patients fitted with an annuloplasty ring. J Heart Valve Dis 1997;6:43–7. [PubMed: 9044075]

5. Ryan LP, Jackson BM, Hamamoto H, Eperjesi TJ, Plappert TJ, St John-Sutton M, Gorman RC, Gorman JH 3rd. The influence of annuloplasty ring geometry on mitral leaflet curvature. Ann Thorac Surg 2008;86:749–60. discussion 749–60. [PubMed: 18721556]
6. Lai DT, Timek TA, Dagum P, Green GR, Glasson JR, Daughters GT, Liang D, Ingels NB Jr, Miller DC. The effects of ring annuloplasty on mitral leaflet geometry during acute left ventricular ischemia. J Thorac Cardiovasc Surg 2000;120:966–75. [PubMed: 11044323]
7. Salgo IS, Gorman JH 3rd, Gorman RC, Jackson BM, Bowen FW, Plappert T, St John Sutton MG, Edmunds LH Jr. Effect of annular shape on leaflet curvature in reducing mitral leaflet stress. Circulation 2002;106:711–7. [PubMed: 12163432]
8. Votta E, Maisano F, Bolling SF, Alfieri O, Montevecchi FM, Redaelli A. The Geoform disease-specific annuloplasty system: a finite element study. Ann Thorac Surg 2007;84:92–101. [PubMed: 17588392]
9. Sacks MS, Enomoto Y, Graybill JR, Merryman WD, Zeeshan A, Yoganathan AP, Levy RJ, Gorman RC, Gorman JH 3rd. In-vivo dynamic deformation of the mitral valve anterior leaflet. Ann Thorac Surg 2006;82:1369–77. [PubMed: 16996935]
10. Green GR, Dagum P, Glasson JR, Nistal JF, Daughters GT 2nd, Ingels NB Jr, Miller DC. Restricted posterior leaflet motion after mitral ring annuloplasty. Ann Thorac Surg 1999;68:2100–6. [PubMed: 10616984]
11. Timek TA, Liang D, Daughters GT, Ingels NB Jr, Miller DC. Effect of semi-rigid or flexible mitral ring annuloplasty on anterior leaflet three-dimensional geometry. J Heart Valve Dis 2008;17:149–54. [PubMed: 18512484]
12. Timek TA, Dagum P, Lai DT, Liang D, Daughters GT, Tibayan F, Ingels NB Jr, Miller DC. Tachycardia-induced cardiomyopathy in the ovine heart: mitral annular dynamic three-dimensional geometry. J Thorac Cardiovasc Surg 2003;125:315–24. [PubMed: 12579100]
13. Bothe W, Chang PA, Swanson JC, Itoh A, Arata K, Ingels NB, Miller DC. Releasable annuloplasty ring insertion--a novel experimental implantation model. Eur J Cardiothorac Surg 2009;36:830–2. [PubMed: 19646892]
14. Bothe W, Kvitting JPE, Swanson JC, Hartnett S, Ingels NB, Miller DC. Effects of Different Annuloplasty Rings on Anterior Mitral Leaflet Dimensions. J Thorac Cardiovasc Surg. 2010 accepted for publication.
15. Glasson JR, Komeda M, Daughters GT 2nd, Bolger AF, Ingels NB Jr, Miller DC. Loss of three-dimensional canine mitral annular systolic contraction with reduced left ventricular volumes. Circulation 1996;94:II152–8. [PubMed: 8901737]
16. Niczyporuk MA, Miller DC. Automatic tracking and digitization of multiple radiopaque myocardial markers. Comput Biomed Res 1991;24:129–42. [PubMed: 2036779]
17. Caimmi PP, Diterlizzi M, Grossini E, Kapetanakis EI, Gavinelli M, Carriero A, Vacca G. Impact of prosthetic mitral rings on aortomitral apparatus function: a cardiac magnetic resonance imaging study. Ann Thorac Surg 2009;88:740–4. [PubMed: 19699889]
18. Bothe W, Nguyen TC, Roberts ME, Timek TA, Itoh A, Ingels NB Jr, Miller DC. Presystolic mitral annular septal-lateral shortening is independent from left atrial and left ventricular contraction during acute volume depletion. Eur J Cardiothorac Surg. 2009
19. Jensen H, Jensen MO, Smerup MH, Vind-Kezunovic S, Ringgaard S, Andersen NT, Vestergaard R, Wierup P, Hasenkam JM, Nielsen SL. Impact of papillary muscle relocation as adjunct procedure to mitral ring annuloplasty in functional ischemic mitral regurgitation. Circulation 2009;120:S92–8. [PubMed: 19752392]
20. Marwick TH, Stewart WJ, Currie PJ, Cosgrove DM. Mechanisms of failure of mitral valve repair: an echocardiographic study. Am Heart J 1991;122:149–56. [PubMed: 2063735]
21. Bothe W, Swanson JC, Ingels NB, Miller DC. How much septal-lateral mitral annular reduction do you get with new ischemic/functional mitral regurgitation annuloplasty rings? J Thorac Cardiovasc Surg. 2010 [Epub ahead of print].
22. Nakatani S, Schwammenthal E, Lever HM, Levine RA, Lytle BW, Thomas JD. New insights into the reduction of mitral valve systolic anterior motion after ventricular septal myectomy in hypertrophic obstructive cardiomyopathy. Am Heart J 1996;131:294–300. [PubMed: 8579024]

23. Jiang L, Levine RA, King ME, Weyman AE. An integrated mechanism for systolic anterior motion of the mitral valve in hypertrophic cardiomyopathy based on echocardiographic observations. Am Heart J 1987;113:633–44. [PubMed: 3825854]

24. Levine RA, Vlahakes GJ, Lefebvre X, Guerrero JL, Cape EG, Yoganathan AP, Weyman AE. Papillary muscle displacement causes systolic anterior motion of the mitral valve. Experimental validation and insights into the mechanism of subaortic obstruction. Circulation 1995;91:1189–95. [PubMed: 7850958]

25. He S, Hopmeyer J, Lefebvre XP, Schwammenthal E, Yoganathan AP, Levine RA. Importance of leaflet elongation in causing systolic anterior motion of the mitral valve. J Heart Valve Dis 1997;6:149–59. [PubMed: 9130123]

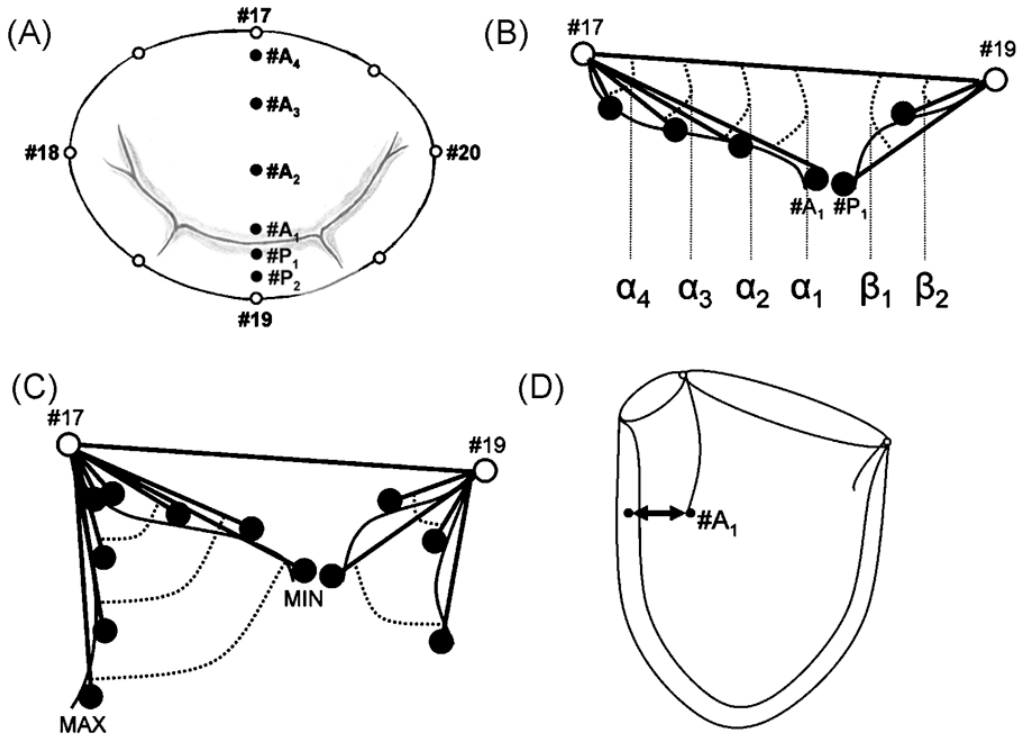

Fig 1.

A: Array of mitral annular (MA), anterior ($\#A_1$–$\#A_4$) and posterior ($\#P_1$–$\#P_2$) mitral leaflet markers; B: Determination of regional anterior and posterior mitral leaflet angles; C: Calculation of regional excursion angles; D: Assessment of anterior mitral leaflet edge ($\#A_1$) to LV septum distance.

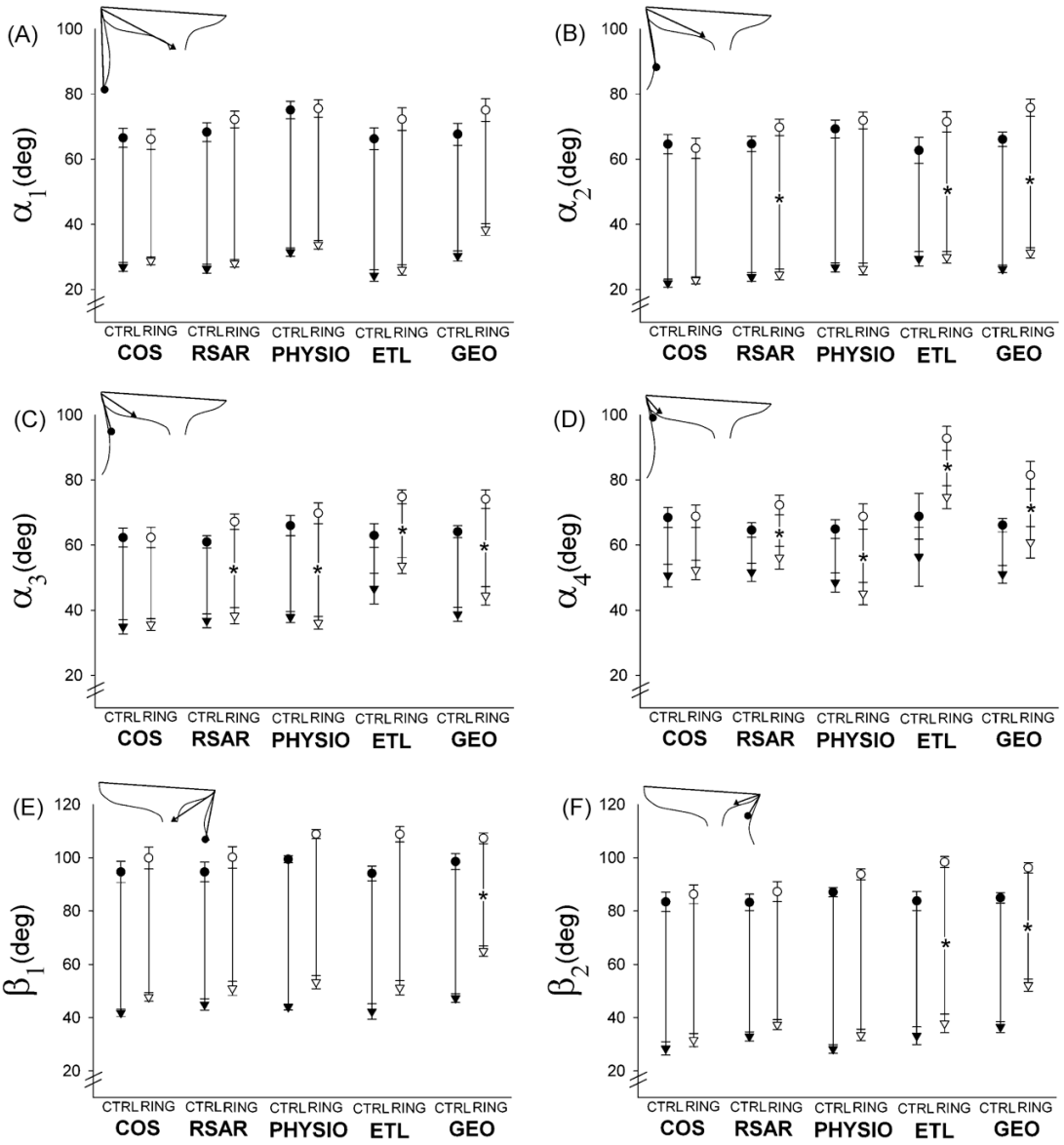

Fig 2.

Minimum (triangles) and maximum (circles) regional anterior (A–D) and posterior (E–F) mitral leaflet angles in the five ring groups with (open symbols) and without (closed symbols) the respective ring inserted. Asterisks indicate that leaflet excursion (maximum minus minimum leaflet angle, see METHODS) for the respective leaflet angle is significantly smaller ($p<0.05$) compared to CTRL (see Table 2).

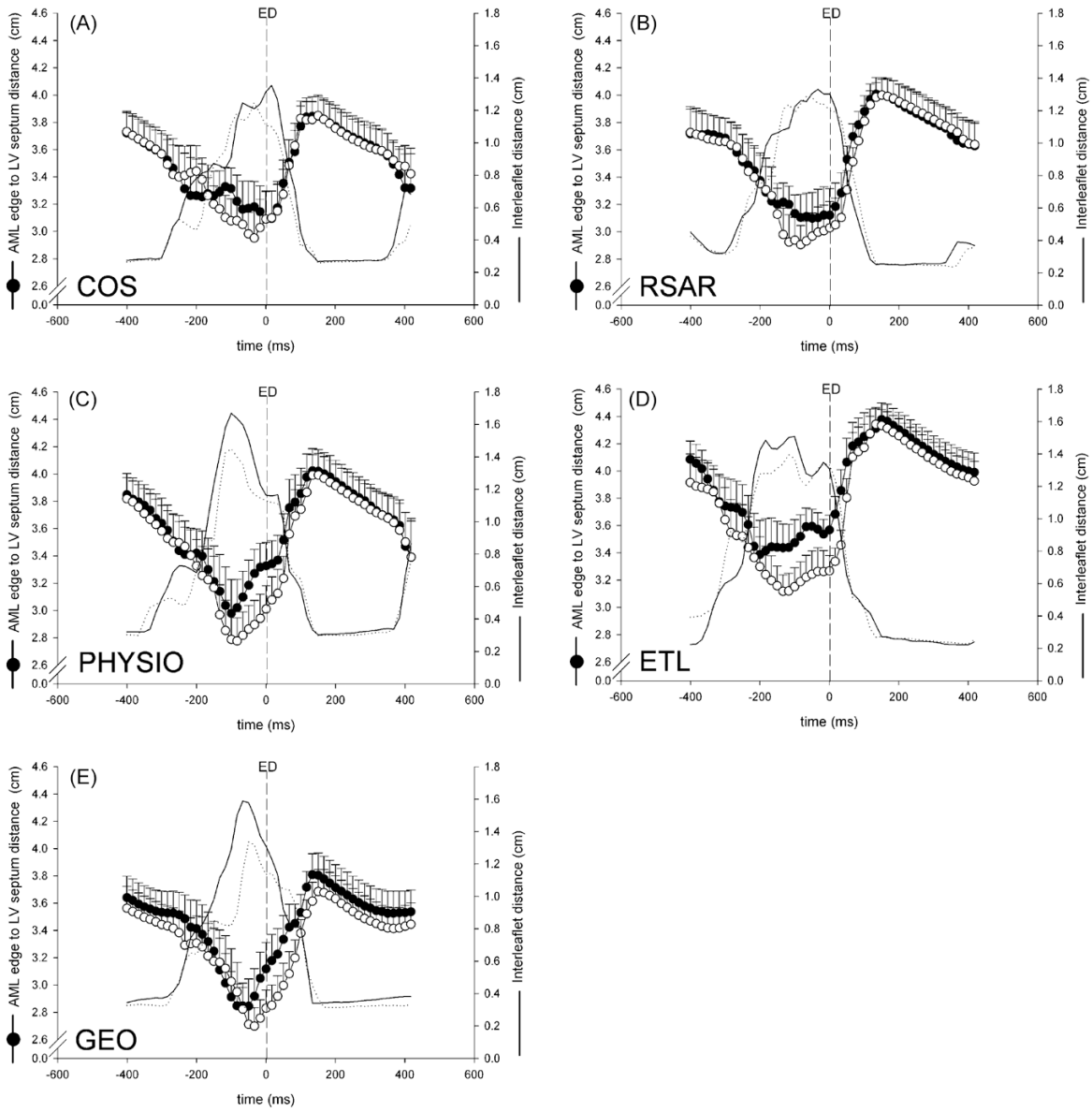

Fig 3.

Distance from anterior mitral leaflet (AML) to LV septum (circles), as well as inter-leaflet distance (lines) plotted throughout the cardiac cycle around end diastole (ED) for COS (A), RSAR (B), PHYSIO (C), ETL (D) and GEO (E) with (open symbols, dotted line) and without (closed symbols, solid line) the annuloplasty ring inserted.

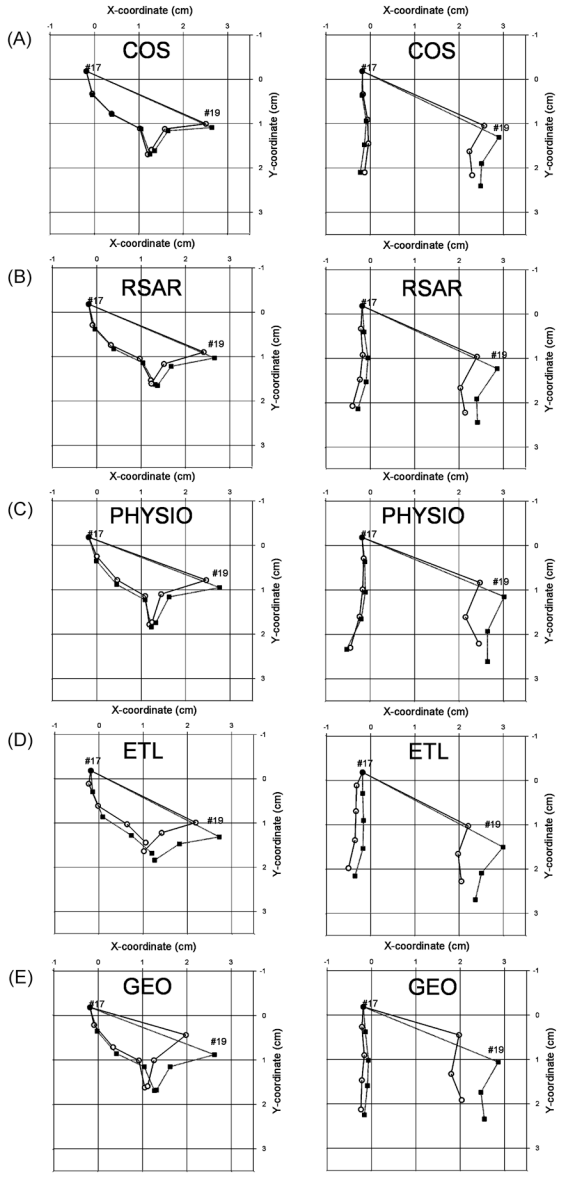

Fig 4.

3-D marker coordinates of mitral annular saddlehorn (#17) and mid-lateral markers (#19), as well as anterior and posterior mitral leaflet markers plotted onto the xy-plane at mid-systole (left column) and at maximum opening (right column) with the saddlehorn marker as the origin of a right-handed cartesian coordinate system (see methods for details). Data are mean values from all animals (A: COS (n=12), B: RSAR (n=12), C: PHYSIO (n=12), D: ETL (n=10), E: GEO (n=12)).

TABLE 1

amics

	COS-Control	COS	p	F	RSAR-Control	RSAR	p	F	PHYSIO-Control	Physio	p	F	ETL-Control	ETL	p	F	GEO-Control	GEO	p	F
	98±13	98±13	.914	.0	89±17	89±15	.853	.0	92±12	92±11	.517	.5	82±6	81±10	.533	.4	92±10	93±10	.492	.5
l)	120±14	121±16	.392	.8	121±22	121±20	.714	.1	123±22	124±21	.934	.0	124±21	125±21	.680	.2	114±14	113±13	.439	.6
mHg/sec)	1360±317	1527±386	.001	19.2	1283±409	1226±297	.340	1.0	1309±333	1348±338	.541	.4	1165±387	1189±382	.217	1.8	1313±315	1388±410	.068	4.1
mHg)	96±8	97±6	.220	1.7	100±9	98±5	.144	2.5	95±8	95±6	.945	.0	94±5	96±4	.109	3.2	96±8	97±7	.617	.3

1 SD, HR=heart rate, LVEDV=left ventricular end diastolic volume, dP/dt_{max}=maximum positive rate of change of left ventricular pressure, LVP_{max} = maximum left ventricular pressure,
s Cosgrove band, RSAR=St Jude Medical rigid saddle-shaped annuloplasty ring, ETL= Edwards IMR ETlogix, GEO=Edwards GeoForm

TABLE 2

otion with annuloplasty rings

	COS-Control	COS	p	F	RSAR-Control	RSAR	p	F	PHYSIO-Control	Physio	p	F	ETL-Control	ETL	p	F	GEO-Control	GEO	p	F
g	2.39±0.38	2.10±0.40	.003	14.8	2.31±0.50	2.17±0.39	.073	3.9	2.70±0.25	2.45±0.24	.004	13.1	2.40±0.36	2.20±0.36	.040	5.7	2.38±0.63	1.97±0.54	.001	19.0
g)	40±8	37±8	.174	2.1	42±8	44±8	.095	3.3	43±8	41±6	.257	1.4	42±11	46±10	.141	2.6	39±9	38±8	.657	.2
s)	91±25	90±23	.877	.0	95±20	102±23	.025	6.7	103±19	97±22	.402	.8	86±29	99±30	.004	14.3	82±27	78±28	.439	.6
s)	59±14	60±15	.947	.0	56±19	73±21	.001	17.8	56±11	59±16	.541	.4	60±17	88±12	.005	13.5	55±24	58±21	.601	.3
g)	43±9	41±9	.306	1.1	41±10	45±10	.006	11.8	42±8	45±6	.074	3.9	33±13	42±14	.003	17.0	39±6	44±6	.012	9.0
s)	81±25	81±22	.970	.0	83±24	90±25	.057	4.5	87±16	91±18	.428	.7	63±33	77±33	.001	22.8	74±12	81±16	.082	3.7
s)	74±17	67±16	.030	6.2	54±18	71±20	.002	16.8	64±20	78±19	.031	6.1	44±16	68±23	.007	11.9	65±22	83±25	.013	8.8
g)	27±11	27±10	.691	.2	24±9	29±11	.002	16.3	28±10	33±10	.006	11.5	16±9	21±12	.006	13.1	25±7	29±9	<.001	25.7
s)	48±24	50±22	.765	.1	43±21	51±23	.003	13.7	52±22	65±25	.009	10.1	24±17	33±23	.006	13.1	40±15	47±18	.006	11.5
s)	41±14	42±18	.848	.0	31±11	39±15	.003	13.8	42±14	48±15	.104	3.1	24±11	31±17	.038	5.9	37±12	46±20	.016	8.2
g)	18±8	17±7	.536	.4	13±6	16±7	.028	6.4	16±7	23±10	.004	13.6	12±4	18±9	.041	5.7	15±5	20±9	.018	7.8
s)	27±18	24±13	.600	.3	19±10	27±15	.016	7.9	23±11	43±26	.003	15.0	18±8	22±10	.044	5.5	20±7	28±17	.014	8.5
s)	29±18	26±10	.605	.3	19±7	23±9	.082	3.7	29±20	34±16	.354	.9	16±6	32±23	.033	6.3	23±8	31±17	.118	2.9
g)	53±13	52±15	.675	.2	50±13	49±10	.846	.0	55±5	55±7	.958	.0	52±8	58±6	.069	4.3	53±5	43±6	.003	14.5
s)	123±31	129±35	.501	.5	121±31	117±23	.558	.5	133±7	128±17	.335	1.0	111±27	131±24	.004	15.2	119±19	103±21	.023	7.0
s)	88±26	73±24	.084	3.6	69±31	67±23	.786	.1	77±18	86±19	.325	1.1	72±16	96±23	.033	6.3	79±31	67±26	.312	1.1
g)	55±16	55±15	.847	.0	50±9	50±13	.883	.0	59±5	60±5	.338	.3	51±8	61±13	.010	10.4	48±9	44±11	.019	7.6
s)	108±36	121±35	.054	4.6	91±24	100±33	.169	2.2	116±16	131±26	.125	2.8	85±23	127±36	.004	15.2	89±22	78±30	.101	3.2
s)	101±44	78±25	.098	3.3	71±29	68±22	.707	.1	90±22	84±17	.255	1.4	66±18	77±20	.213	1.8	82±29	70±30	.149	2.4

COS=Edwards Cosgrove band, RSAR=St Jude Medical rigid saddle-shaped annuloplasty ring, ETL= Edwards IMR ETlogix, GEO=Edwards GeoForm, VO_{max} = maximum opening
ximum closing velocity, see METHODS for details